Performance Comparison of Single- and Two-Loop Control Systems on a Rotary Table

B. Özkan
The Scientific and Technological Research Council of Turkey,
Defense Industry Research and Development Institute, Ankara, Turkey

ABSTRACT

The control of the rotary platforms is one of the important issues in the control engineering. Depending on the application area considered, the accuracy level of the relevant control systems may become higher. However, the undesired external inputs such as sensor noise and base vibrations have diverting effects on the on the plant, or the system to be controlled and hence the regarded performance requirments may not be achieved in many cases. In order to overcome this problem, robust control system architectures are constructed rather than classical control systems as well as other modern and advanced control approaches such as neural network based and fuzzy control systems. In this study, a two-loop control structure is proposed in order to improve the control quality of the handled rotary table and the results of the relevant computer simulations are presented in addition to the data collected from the simulations conducted on the single-loop control system. Eventually, it is shown that the two-loop control system gives more satisfactory results than the conventional single-loop control system.

Keywords: Single-loop control system, two-loop control system, rotary table

INTRODUCTION

In order to simulate the performance characteristics of the critical mechatronics devices in the real environment, the hardware-in-the-loop (HWIL) simulators are utilized in most of the applications. These simulators provide an opportunity to the developers with making necessary design updates prior to the production of the mentioned mechatronic devices as well as reducing the total cost at a significant level [1].

Since their moving platforms are usually rotary-type, the control of the rotary tables or gimbals become one of the most important issues in the design of the HWIL motion simulators. In this sense, several control schemes have been proposed in accordance with

convenient control actions. Namely, the neural network type, fuzzy logic based and robust control systems are designed as alternatives to classical control systems regarding PI (proportional plus integral) or PID (proportional plus integral plus derivative) control action in order to improve the system performance [2].

Looking at the literature, it is seen that the conventional control systems designed for rotary configurations are in general single-loop algorithms based on the angular position control. On the other hand, although they are not so common as the single-loop ones, the two-loops control systems have also been designed in order to increase the positioning accuracy [3]. In the mentioned algorithm, the outer loop makes the position control of the considered gimbal to compensate the steady-state position error while the inner loops tries to nullify the angular speed of the gimbal within the presumed settling time [4].

In this study, the precise control of a rotary table is dealt with and the relevant single- and two-loop control algoritms are constructed. While the single-loop control system accounts the classical PID control action, the PIV (proportional plus integral plus velocity) rule is utilized for the speed control system in the inner loop along with the outer position control loop regarding the PI law in the two-loop counterparts. At the final part of the study, the results conducted from the related computer simulations are evaluated.

SYSTEM MODEL

The schematic representation of the rotary table model considered is as shown in Figure 1. As indicated, the system consists of the rotary table which is used to provide the considered test item with the planned angular motion, a DC-type servomotor, the connecting shaft between the table and motor, support bearings, and the fixed frame of the structure. Here, a direct-drive connection is established between the motor and connecting shaft. Also, the encoder onboard the motor is used as the feedback device of the designed control systems.

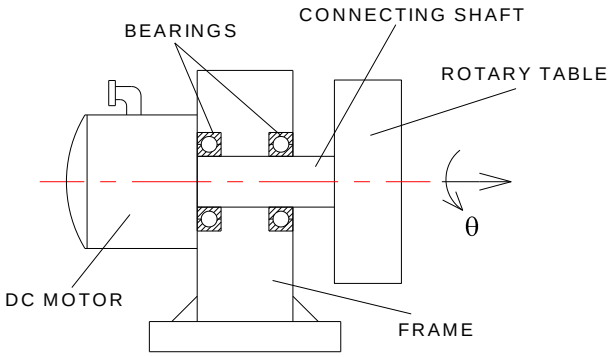

Figure 1. Rotary Table Model

From here, as θ denotes the relevant angular position variable, the dynamics of the rotary table can be described in the following manner:

$$J_e \ddot{\theta} + B_e \dot{\theta} = T_m \quad (1)$$

where J_e, B_e, and T_m stand for the equivalent moment of inertia of the rotary table, connecting shaft, inner bearing rings, and rotor of the DC motor of the connecting shaft, equivalent viscous friction coefficient representing the frictional effects on the bearings and rotor, and control torque applied by the torque motor, respectively.

CONTROL SYSTEM DESIGN

Single-Loop Control System

In the PID type controller which is the most preferably used controller in the industry because of its simplicity and ease of implementation, the control signal to be sent to the plant, or the system to be controlled, is generated by multiplying the error between the desired and actual values of the control variable, sum of the error within a certain interval, and error rate with the proportional (P), integral (I), and derivative (D) gains. Here, the mentioned gains are chosen in accordance with the desired behavior of the control system. In this scheme, the integral action tries to nullify the steady-state error on the control variable which results from the parameter uncertainties, disturbances, and noises while the derivative action handles the trends in the transient error [5]. The block diagram of the control system with the PID controller is given in Figure 2. In this scheme, K_c and K_t represent the driver gain and motor torque constant while θ_d, E, I_c, and I show the desired value of the control variable, error term, controller output, and driving current to the motor, respectively. Also, $G_c(s)$ indicates the controller transfer function as "s" denotes the Laplace operator.

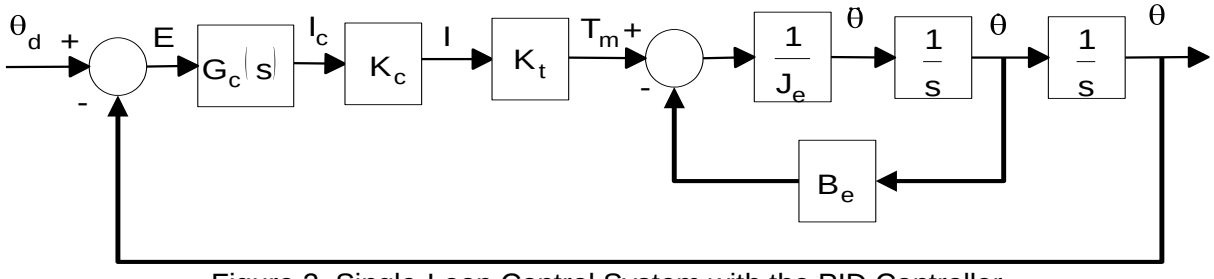

Figure 2. Single-Loop Control System with the PID Controller

According to the PID law, $G_c(s)$ can be established as follows:

$$G_c(s) = K_p + \frac{K_i}{s} + K_d s \quad (2)$$

where K_p, K_i, and K_d denote the proportional, integral, and derivative gains, respectively.

Simplifying the scheme in Figure 2 using the block diagram algebra, the closed-loop transfer function from θ_d to θ is obtained as given below:

$$\frac{\theta(s)}{\theta_d(s)} = \frac{n_2 s^2 + n_1 s + 1}{d_3 s^3 + d_2 s^2 + d_1 s + 1} \tag{3}$$

where $n_1 = K_p / K_i$, $n_2 = K_d / K_i$, $d_1 = K_p / K_i$, $d_2 = (B_e / K_c K_t K_i) + (K_d / K_i)$, and $d_3 = J_e / (K_c K_t K_i)$.

After getting the transfer function of the closed-loop control system as in equation (3), the roots of the relevant characteristic polynomial, i.e. the poles of the control system, can be placed according to the specified performance requirements and thus the corresponding controller gains can be determined. One of the methods available for pole placement is to locate the poles by means of certain polynomials such as Butterworth and Chebyshev polynomials. This way, it becomes possible to decide on the poles such that the control system attains the desired bandwidth [6]. Here, the Butterworth polynomials leading mimimum overshoot values in the system response are considered. Hence, the following third-order Butterworth polynomial can be used to equate the characteristic polynomial, i.e. the denominator polynomial, of the transfer function in equation (3) [7]:

$$B_3(s) = \frac{s^3}{\omega_c^3} + \frac{2 s^2}{\omega_c^2} + \frac{2 s}{\omega_c} + 1 \tag{4}$$

where ω_c shows the desired bandwidth value of the control system in rad/s.

Matching the mentioned characteristic polynomial in equation (3) to equation (4) and making the intermediate calculations, the following expressions are held for K_p, K_i, and K_d:

$$K_p = 2 J_e \omega_c^2 / (K_c K_t) \tag{5}$$

$$K_i = J_e \omega_c^3 / (K_c K_t) \tag{6}$$

$$K_d = (2 J_e \omega_c - B_e) / (K_c K_t) \tag{7}$$

Two-Loop Control System

The two-loop control system structure whose schematic representation is shown in Figure 3 consists of two control systems one of which operates inside the other. In this algorithm, the outer control loop attempts the rotary table to bring to the desired position while the inner loop which is at least four times faster than the outer one in order not to affect its dynamics is designated to make the angular speed of the gimbal zero. Here, the outer loop controller symbolized with $G_c(s)$ is constructed according to the classical PI control law

whereas the PIV type controller is employed in the inner loop, or speed control system, shown by $G_v(s)$ in order to minimize the diversing effects of the disturbing inputs.

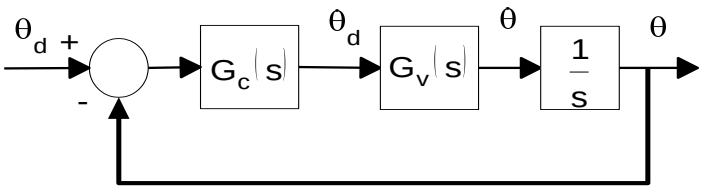

Figure 3. Two-Loop Control System Structure

Thus, as K_p and K_i stand for the proportional and integral gains, the position controller of the outer loop can be modeled in the following fashion:

$$G_c(s) = K_p + \frac{K_i}{s} \tag{8}$$

From here, the closed-loop transfer function of the outer loop is obtained as K_0 indicates the steady-state gain of the inner loop:

$$\frac{\theta(s)}{\theta_d(s)} = \frac{n_1 s + 1}{d_2 s^2 + d_1 s + 1} \tag{9}$$

where $n_1 = d_1 = K_p / K_i$ and $d_2 = 1/(K_0 K_i)$.

Also, the second-order Butterworth polynomial can be formulated as follows:

$$B_2(s) = \frac{s^2}{\omega_c^2} + \frac{\sqrt{2}\, s}{\omega_c} + 1 \tag{10}$$

Hence, equating the characteristic polynomial of the transfer function in equation (9) to the polynomial in equation (10), the expressions giving K_p and K_i are obtained as given below [7]:

$$K_p = \sqrt{2}\, \omega_c / K_0 \tag{11}$$

$$K_i = \omega_c^2 / K_0 \tag{12}$$

The block diagram of the speed control system shown by $G_v(s)$ in Figure 3 can be built with respect to the PIV control law as given in Figure 4. In this scheme, it is assumed that the necessary angular acceleration information is gotten by taking the time derivative of the angular velocity measurement. In fact, this is not applicable in real-time implementation due to the noise effects on the acquired data. Hence, the use of a conveniently-designed estimator is more suitable in such cases.

PIV type controller which is often implemented in the control of electric motors is another kind of the classical controllers formed by modifying the PID structure. In the PIV controller, the position feedback is combined with the velocity feedback [8]. Unlike the PID controller, the position error (e) is turned into the velocity command by multiplying it with the position gain (K_p) and the integral gain (K_i) operates on the velocity error rather than the

position error in this algorithm. Moreover, the velocity gain (K_v) is introduced instead of the derivative gain in the PID law (K_d) [9]. Here, the necessary velocity information is provided either by means of a speed sensor or using an estimator.

From Figure 4, the transfer function of the closed-loop speed control system is obtained as follows:

$$\frac{\dot{\theta}}{\dot{\theta}_d} = \frac{1}{d_2 s^2 + d_1 s + 1} \tag{13}$$

where, for $\gamma = 1/(K_c K_t K_p K_i)$, $d_1 = \gamma (B_e + K_c K_t K_i)$ and $d_2 = \gamma (J_e + K_c K_t K_v)$.

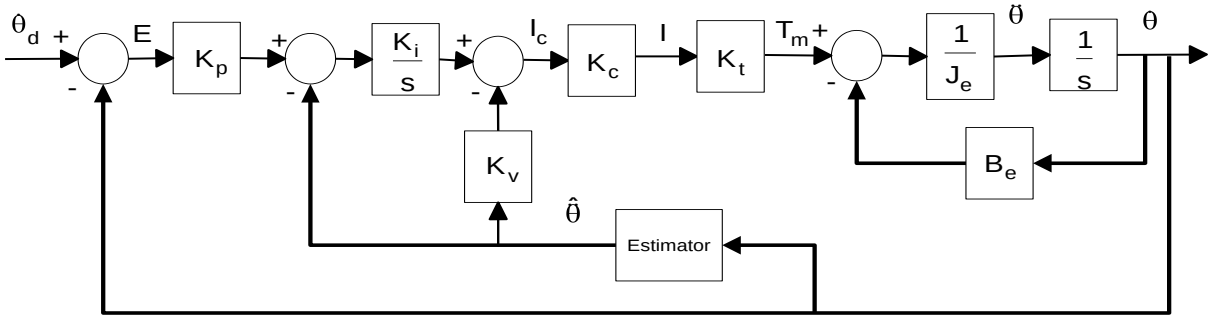

Figure 4. Speed Control System with the PIV Controller

As seen, the characteristic polynomial of the transfer function given in equation (13) possesses two roots. In the case of finding the controller gains using a second-order Butterworth polynomial, two equations will arise for three parameters. Here, the required parameters, i.e. controller gains, can be calculated by means of certain formulas or some amprical approaches [5]. On the other hand, sufficient number of equations to solve the parameters can be established by increasing the order of the control system with some small changes. Namely, as $-1/T_s$ is an extraneous root sufficiently small compared to the original roots of the control system, the parameter K_v can be modified as $K_v/(T_s s + 1)$. Using this low-pass filter with the corner frequency at $1/T_s$, the frequency range within which K_v is effective is also restricted and hence the effects of the high-frequency noise on the derivative action can be minimized [5]. Making this modification, equation (17) takes the following form:

$$\frac{\dot{\theta}}{\dot{\theta}_d} = \frac{T_s s + 1}{d_3 s^3 + d_2 s^2 + d_1 s + 1} \tag{14}$$

where, for $\gamma = 1/(K_c K_t K_p K_i)$, $d_1 = \gamma (B_e + K_c K_t K_i (T_s K_i + 1))$, $d_2 = \gamma (J_e + T_s B_e + K_c K_t (K_v + T_s K_i))$, and $d_3 = J_e T_s \gamma$.

If noticed, the control system with the modified PIV controller has a zero at $z = -1/T_s$ whereas the system with the original PIV does not have a zero dynamics. Conversely, putting $-1/T_s$ at least 100 times far away from the system root at the farest location with

respect to the origin such that it does not affect the overall system dynamics, the existence of this zero will not cause any undesired result.

Eventually, equating the characteristic polynomial of the transfer function given in equation (14) to the third-order Butterworth polynomial in equation (4), as f_s denotes the desired bandwidth of the control system (in Hertz) and $\omega_s = 2\pi f_s$, K_p, K_i, and K_v are determined as given below:

$$K_p = \omega_s / (2 - T_s \omega_s) \tag{15}$$

$$K_i = J_e T_s \omega_s^2 (2 - T_s \omega_s) / (K_c K_t) \tag{16}$$

$$K_v = [J_e (T_s \omega_s - 1)(T_s^2 \omega_s^2 - T_s \omega_s - 1) - T_s B_e] / (K_c K_t) \tag{17}$$

COMPUTER SIMULATIONS

In order to evaluate the performances of the proposed control systems, the relevant computer simulations are conducted in the MATLAB© SIMULINK© environment. The numerical values of the parameters given in Table 1 are obtained from the related technical documents. Also, the constructed control system models are converted into their discretized forms using the Tustin method [5].

Table 1. Numerical Values Used in the Simulations

Parameter	Numerical Value
J_e (kg · m²)	1.25
B_e (N · m · s / rad)	0.1
f_c (Hz)	5
f_s (Hz)	20
K_c (A / V)	1
K_t (N · m / A)	25
T_s (s)	1/500
Simulation Sampling Frequency (Hz)	2000
Resolver Resolution (bit)	16

Regarding the data in Table 1, the responses of the single- and two-loop control systems are plotted against a reference input of 1° as shown in Figure 5 and Figure 6. In this sense, Figure 7 shows the response characteristic of the inner controller of the designed two-loop control system. In all cases, it is assumed that the control systems are subjected to the encoder noise at the maximum amount of 0.05° in both directions.

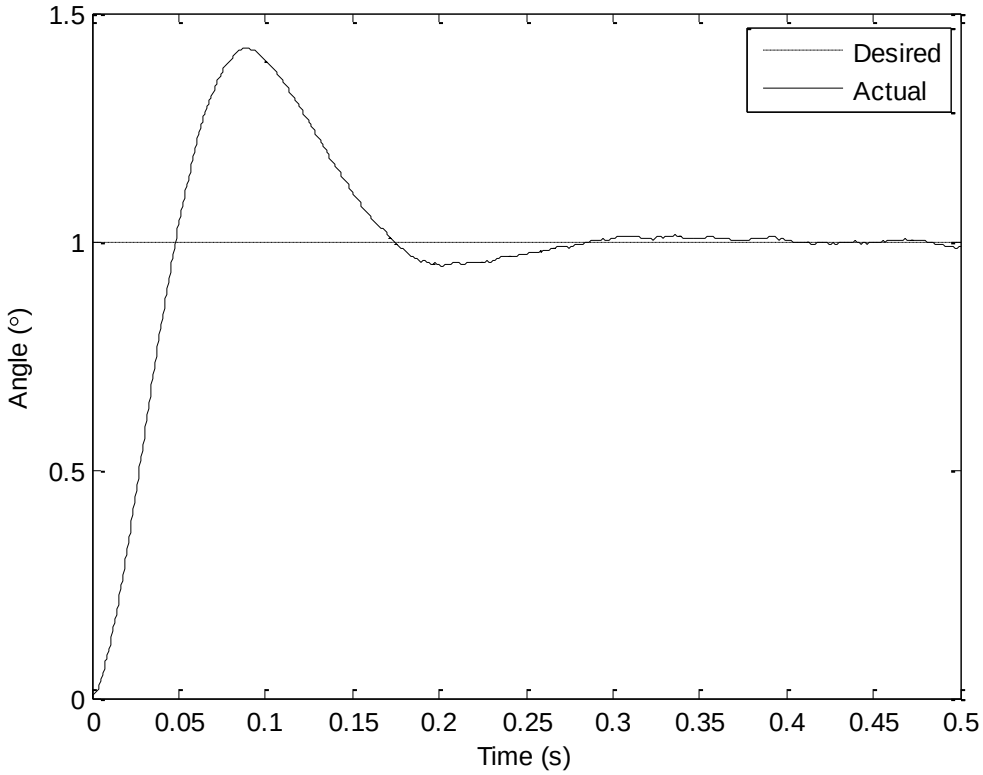

Figure 5. Unit Step Response of the Single-Loop Control System with the PID Controller

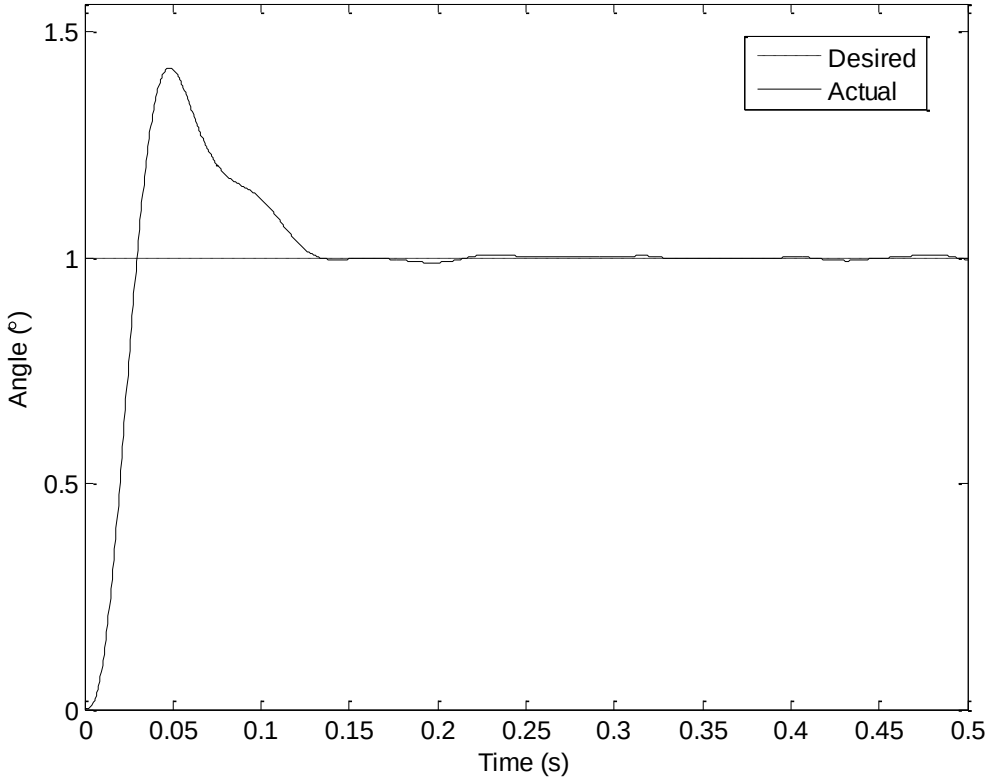

Figure 6. Unit Step Response of the Two-Loop Control System with the PIV Type Speed Controller

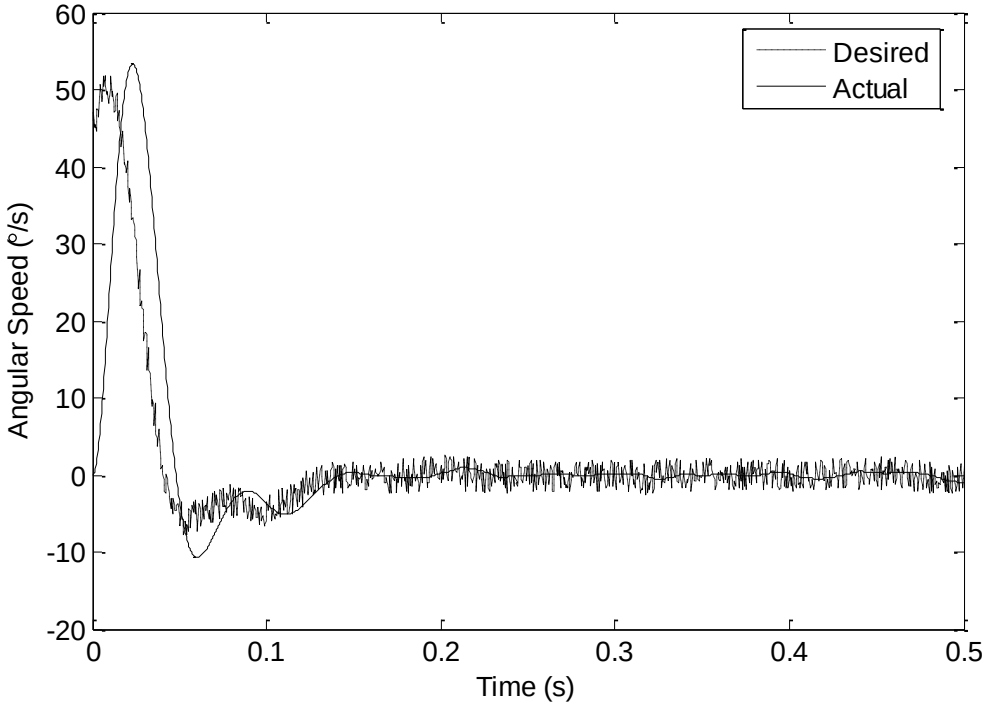

Figure 7. Response of the Speed Control System with the PIV Controller

At the end of the computer simulations, the maximum current requirement, maximum overshoot, settling time, and maximum oscillation quantities are obtained for both types of the control systems as given in Table 2. Also, the steady-state error occurs as zero in both cases.

Table 2. Simulation Results of the Single-Loop Control Systems

Control System	**Maximum Current Requirement (A)**	**Maximum Overshoot (%)**	**Settling Time (ms)**	**Maximum Amplitude of Oscillations (μrad)**
Single-Loop	10.31	42.4	200	245
Two-Loop	3.19	42.1	118	185

DISCUSSION AND CONCLUSION

When the responses of the single- and two-loop control systems designed for a rotary table, it is seen that the two-loop one yields smaller results in the sense of the maximum current requirement, overshoot, and steady-state oscillations as well as the settling time. That is because the speed of the plant is regulated via the inner loop in the two-loop structure. This also leads the undesired noise effects on the encoder to be suppressed prior to influencing the angular position response of the entire control system. On the other hand, the proposed algorithm for the two-loop control system is more complex than its single-loop counterpart. Unlike the conventional single-loop configuration, the two-loop variant requires a

well-designed estimator to calculate the angular speed and acceleration of the table accurately.

REFERENCES

[1] Page, J. L. and Willis, K. E., *"Designing Motion Systems for Hardware-in-the-Loop Simulation"*, Carco Electronics Publication, USA, 1998.

[2]. Wu, Y., Le, W. and Tian, D., *"Application of Sliding Mode Control Based on Disturbance Observer on High Performance Flight Motion Simulator"*, Proceedings of the IEEE International Conference on Automation and Logistics, pp. 2695-2699, China, August 2007.

[3]. Murphy, K., Goldblatt, S., Warren, J., Chapman, R., Hemler, J., Mitchell, C., and Moe, G., *"Pointing and Stabilization System for Use in a High Altitude Hovering Helicopter"*, SPIE, Proceedings of the Conference on Acquisition, Tracking, and Pointing XIII, ABD, Vol. 3692, pp. 23-32, 1999

[4]. Smith, B. J., Schrenk, W. J., Gass, W. B., and Shtessel, Y. B., *"Sliding Mode Control in a Two Axis Gimbal System"*, Proceedings of IEEE Aerospace Conference, pp. 457-470, March 6-13, 1999

[5]. Özkan, B., Yıldız, E. N., and Dönmez, B., *"Precise Position Control of a Gimbaled Camera System"*, AIAA Guidance, Navigation, and Control Conference and Exhibit, Honolulu, Hawaii, USA, August 2008

[6]. Lee, C. H., *"A Survey of PID Controller Design based on Gain and Phase Margins"*, International Journal of Computational Cognition, Vol. 2, No. 3, pp. 63-100, September 2004

[7]. Özkan, B., *Dynamic Modeling, Guidance and Control of Homing Missiles*, PhD Thesis, Mechanical Engineering Department, Middle East Technical University, Turkey, 2005

[8]. Zhang, R. and Chen, Y., *"Dual-Loop Feedback Control of Servo Motor Systems Using Singular Perturbation Methods"*, Proceedings of the American Control Conference, Denver, Colorado, USA, pp. 4567-4662, June 4-6, 2003

[9]. Kaiser, D., *"Fundamentals of Servo Motion Control"*, Technical Report of Parker Compumotor, 2001